Cluster-glass behavior of a highly oxygen deficient perovskite, $BaBi_{0.28}Co_{0.72}O_{2.2}$

2009 J. Phys.: Condens. Matter 21 105801

(http://iopscience.iop.org/0953-8984/21/10/105801)

J. Phys.: Condens. Matter **21** (2009) 105801 (7pp) doi:10.1088/0953-8984/21/10/105801

Cluster-glass behavior of a highly oxygen deficient perovskite, $BaBi_{0.28}Co_{0.72}O_{2.2}$

T Klimczuk[1,2], H W Zandbergen[2,3], Q Huang[4], T M McQueen[2], F Ronning[1], B Kusz[5], J D Thompson[1] and R J Cava[2]

[1] Los Alamos National Laboratory, Los Alamos, NM 87545, USA
[2] Department of Chemistry, Princeton University, Princeton, NJ 08544, USA
[3] National Center for HREM, Department of Nanoscience, Delft University of Technology, Rotterdamseweg 137, 2682 AL Delft, The Netherlands
[4] NIST Center for Neutron Research, NIST, Gaithersburg, MD 20899, USA
[5] Faculty of Applied Physics and Mathematics, Gdansk University of Technology, Narutowicza 11/12, 80-952 Gdansk, Poland

Received 2 December 2008, in final form 25 January 2009
Published 13 February 2009
Online at stacks.iop.org/JPhysCM/21/105801

Abstract
A highly oxygen deficient perovskite, $BaBi_{0.28}Co_{0.72}O_{2.2}$, was synthesized by solid state reaction. The crystal structure was determined by means of neutron and x-ray powder diffraction. The material exhibits semiconducting behavior with an energy gap of 1.8 eV. The electron diffraction study does not reveal long range Bi:Co ordering; instead it shows the existence of short range ordering in this phase. The AC and DC magnetic susceptibility studies reveal cluster-glass behavior, which has its origin in the interacting ferromagnetic clusters present.

(Some figures in this article are in colour only in the electronic version)

1. Introduction

Perovskites have been the focus of intensive research for several decades. With general formula ABX_3, they display a full range of physical properties, such as superconductivity, ferroelectricity, and giant magnetoresistance, and are especially interesting as they often display complex correlations among their structures, chemistry, and physical properties. There are relatively few cobalt oxides that crystallize in the cubic perovskite structure, including for example $LnCoO_3$ (Ln = La, Pr, Nd, Sm) [1], $SrCoO_{2.64}$ [2], and $BaCoO_{2.23}$ [3]. In the latter two compounds, the perovskite structure is stabilized through an increase of the Co size by reduction of its valence and the lowering of its coordination number by removal of some oxygen ions. $BaBiO_3$ and $BaCoO_3$ are well known compounds. $BaBiO_3$ crystallizes in the double perovskite structure, in which corner shared $Bi^{3+}O_6$ and $Bi^{5+}O_6$ octahedra alternate, with Ba^{+2} ions in the cavity positions. $BaCoO_3$, on the other hand, posses a hexagonal non-perovskite structure, consisting of columns of face sharing CoO_6 octahedra separated by Ba^{2+} ions integrated into the close packed O planes. Both materials are semiconductors: $BaBiO_3$ is an unusual charge-density-wave (CDW) semiconductor [4] and $BaCoO_3$ is an n-type semiconductor that shows no long range magnetic ordering [5]. $BaCoO_3$ can be considered as a spin 1/2 material with an effective magnetic moment of approximately $2.3\mu_B$ [6]. The presence of non-interacting ferromagnetic clusters, with a size of about 1.2 nm, has been theoretically predicted for hexagonal $BaCoO_3$ [7].

Our motivation in the present study was to dope the parent $BaBiO_3$ compound with Co to induce ferromagnetism. Although Bi and Co are distinctly different chemically, and random substitution of Co for Bi in a perovskite solid solution is therefore unexpected, we made the $BaBi_{1-x}Co_xO_{3-d}$ series of samples and found that a highly oxygen deficient, perovskite type structure is stable for a small range of intermediate compositions near 75% Co doping. The compound has the formula $BaBi_{0.28}Co_{0.72}O_{2.2}$. We find no evidence for long range Co/Bi ordering, but through electron diffraction see that they are ordered over the short range. The physical properties of this compound, in particular its cluster-glass behavior, are also discussed here.

2. Experiment

Polycrystalline $BaBi_{1-x}Co_xO_{3-\delta}$ samples were prepared by solid state reaction of BaO_2 (Sigma Aldrich 95%), Co_3O_4

(Alfa Aesar 99.7%), and Bi_2O_3 (Alfa Aesar 99.75%). Well ground, pelleted, stoichiometric mixtures of the oxides were fired under flowing high purity nitrogen at a temperature of 825 °C for a total of 7 days. Samples were cooled quickly in the nitrogen flow by removal of the process tube from the furnace. Complete reaction required multiple regrinding and re-heating.

Characterization of the products by room temperature x-ray powder diffraction (XRD) was performed with Cu Kα radiation ($\lambda = 0.154\,60$ nm) in the angular range $10° \leqslant 2\theta \leqslant 90°$ in steps of 0.02° using a Bruker D8 diffractometer, with a graphite diffracted beam monochromator. One sample was examined by neutron powder diffraction. Neutron diffraction data were collected at the NIST Center for Neutron Research on the BT-1 powder neutron diffractometer with neutrons of wavelength 1.5403 Å produced by a Cu(311) monochromator. Collimators with horizontal divergences of 15′ and 20′ of arc were used before and after the monochromator, and a collimator with a horizontal divergence of 7′ was used after the sample. Data were collected in the 2θ range of 3°–168° with a step size of 0.05°. Rietveld refinements of the structures were performed with GSAS [8, 9]. The neutron scattering amplitudes used in the refinements were 0.507, 0.853, 0.249 and 0.581 ($\times 10^{-12}$ cm) for Ba, Bi, Co and O, respectively.

Electron microscopy was performed on electron transparent areas that were obtained by crushing and dropping a suspension of the powder in ethanol on a carbon coated holey film. High resolution electron microscopy (HREM) and electron diffraction were performed with a Philips CM200ST electron microscope with a field emission gun operated at 200 kV and equipped with an EDX (energy dispersive x-ray) element analysis system. The magnetic susceptibility was measured on a powder sample with a SQUID magnetometer (Quantum Design) in the temperature range 5–300 K. Continuous measurement of the electrical conductivity was made in air by the two terminal method (reliable because the resistivity of the material is very high) in the temperature range 400 K $< T <$ 670 K. In that temperature range $BaBi_{0.28}Co_{0.72}O_{2.2}$ remains stable in air.

3. Results

Figure 1 shows the crystallographic cell parameter for the new cubic phase, determined by powder x-ray diffraction, as a function of Co content (x) in the series of $BaBi_{1-x}Co_xO_{3-\delta}$ samples. Initial Co substitution for Bi in $BaBiCo_3$, for $x \leqslant 0.7$, leads to a mixed phase region consisting of two cubic phases: $BaBiO_3$ and $BaBi_{1-x}Co_xO_{3-\delta}$. The unit cell of the new phase, $a = 4.1443(2)$ Å, is slightly bigger than that of perovskite $BaCoO_{2.23}$ ($a = 4.072$ Å) [3]. The fact that it is unchanging in the low x region, and that a mixture of phases is observed for low x, indicates that $BaBi_{1-x}Co_xO_{3-\delta}$ is not a continuous solid solution, and that a distinct phase is found for x near 0.75. Within the new phase, the lattice parameter changes continuously with x, indicating that the cubic compound exists over a range of compositions $BaBi_{1-x}Co_xO_{3-\delta}$ for $0.70 < x \leqslant 0.90$. The inset of figure 1 shows the high angle x-ray diffraction pattern. A clear shift of the high angle

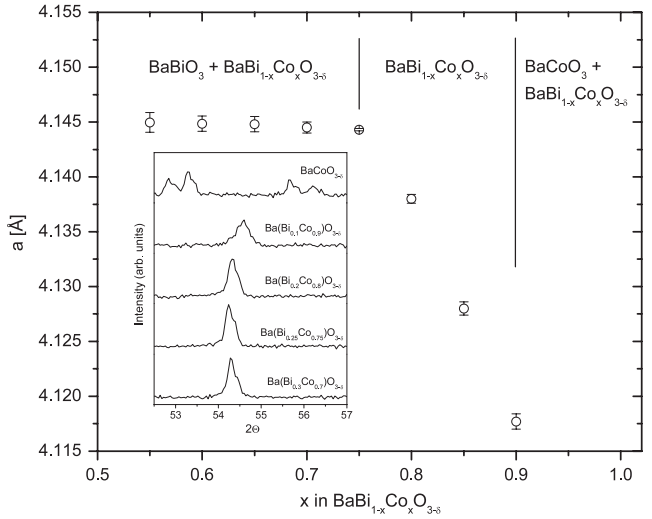

Figure 1. Crystallographic cell parameter a of the $BaBi_{1-x}Co_xO_{3-\delta}$ as a function of x. The inset shows powder x-ray diffraction patterns (Cu Kα) of samples with nominal composition $BaBi_{1-x}Co_xO_{3-\delta}$, $x = 0.7, 0.75, 0.8, 0.85, 0.9, 1$. Three regions are shown: (I) $x < 0.75$ where both phases $BaBiO_3$ and $BaBi_{1-x}Co_xO_{3-\delta}$ are present (II) $0.75 \leqslant x \leqslant 0.9$ where only $BaBi_{1-x}Co_xO_{3-\delta}$ is present and (III) $0.9 < x < 1.0$ where both $BaBi_{0.9}Co_{0.1}O_{3-\delta}$ and $BaCoO_3$ are present.

(221) peak with doping level above 0.75 is observed. The purest sample was obtained for the nominal cation ratio: 4:1:3 ($BaBi_{0.25}Co_{0.75}O_x$) and this sample was employed for the physical property measurements.

Figures 2 and 3 show the $[1\bar{2}1]$ and tilted [111] electron diffraction patterns. The $[1\bar{2}1]$ electron diffraction pattern shows the basic perovskite reflections and, in addition, diffuse scattering in particular at positions that can be described with a vector $\mathbf{q}_1 = (1/2)(\mathbf{a}^* + \mathbf{b}^* + \mathbf{c}^*)$ from each of the main reflections. Apart from these diffuse diffraction spots one can observe diffuse intensity closer to the basic diffraction spots at $\mathbf{q}_2 = (1/6)(\mathbf{a}^* + \mathbf{b}^* + \mathbf{c}^*)$. Given the diffuse nature and the fact that these $\mathbf{q}_2$-type diffuse reflections also stretch out along the viewing direction, it is not useful to give a more precise value of $\mathbf{q}_2$. The vector $\mathbf{q}_1$ indicates a doubling along [111], and is likely due to short range Bi/Co ordering: this type of ordering is known to occur over long ranges in classical double perovskites, even in cases when the B-site metal ratio is not 1:1, such as occurs for $Ba_3MgTa_2O_9$ [10]. The vector $\mathbf{q}_2$ is compatible with a 6 fold spacing along [111], which suggests a relation of this short range ordering to O vacancy ordering. The ∼[111] diffraction pattern was not taken in the exact [111] orientation, to enhance the visibility of the superreflections and allow the determination of the extension of the superreflections away from the exact [111] diffraction plane. The basic reflections in the vertical line through the origin are fully excited, in contrast with the rows of reflections adjacent to this central row. It is clear that the intensity of the diffuse scattering in these adjacent rows is quite strong compared to the basic reflections, indicating that the diffuse superreflections extend much more in the [111] direction than the basic reflections do. One can also observe that the shape

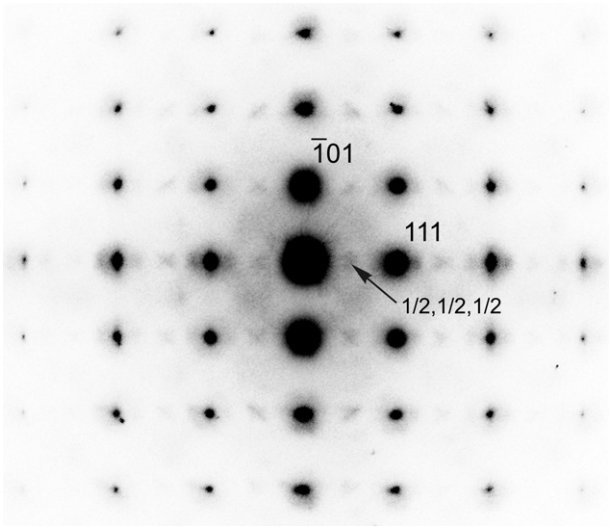

Figure 2. [$1\bar{2}1$] electron diffraction pattern, showing (i) the basic reflections, (ii) weak rather diffuse intensities at positions half way between the basic reflections in the [111] direction (e.g. the reflection 1/2, 1/2, 1/2) and (iii) weak diffuse intensities close to the basic reflections and also in the [111] direction.

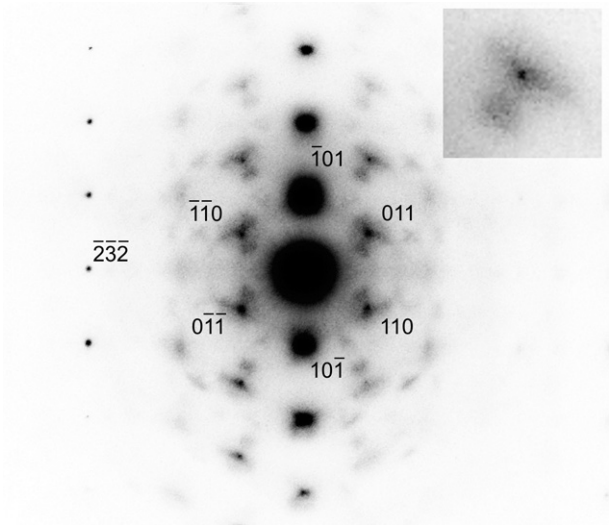

Figure 3. A tilted [111] electron diffraction pattern, with a tilt of 8° about the $\bar{1}01$ direction to enhance the visibility of the diffuse scattering. The basic reflections closest to the central spot are indexed. The inset shows an enlargement of the 011 reflection (the sharp dot) with the diffuse scattering around it.

of the diffuse superreflections is quite complicated, due to the existence of very short range superstructure ordering occurring in various symmetry related (in the basic unit cell) directions.

Rietveld analysis of the neutron powder diffraction data (table 1, figure 4) confirms that the ratio of Bi:Co in the perovskite is close to 1:3, with freely refined occupancies of Bi: 0.28(1), Co: 0.72(1), and O: 2.19(2), yielding a formula $BaBi_{0.28}Co_{0.72}O_{2.2}$. An impurity phase of 3 wt% $BaCoO_3$ was also included in the refinements. This fraction of $BaCoO_3$ is consistent with the refined formula of $BaBi_{0.28}Co_{0.72}O_{2.2}$ for the new phase, given that the ratio of starting materials for

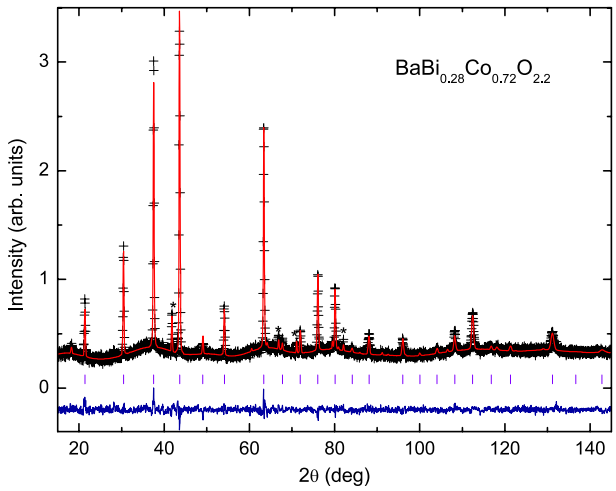

Figure 4. The neutron powder diffraction pattern of the sample of composition $BaBi_{0.28}Co_{0.72}O_{2.2}$. The asterisks mark main peaks of the 3 wt% impurity phase $BaCoO_3$.

Table 1. Crystallographic data for $BaBi_{0.28}Co_{0.72}O_{2.2}$. Space group $Pm\bar{3}m$ (#221). Atomic positions, Ba: 1a(0 0 0), Bi/Co: 1b(1/2 1/2 1/2), O: 3c(0 1/2 1/2).

		$BaBi_{0.28}Co_{0.72}O_{2.2}$
	a (Å)	4.1431(1)
Ba	U	0.045(1)
Bi/Co	N_{Bi}/N_{Co}	0.28(1)/0.72(1)
	U	0.048(1)
O	N	0.731(8)
	$U_{11} = U_{22}$	0.048(1)
	U_{33}	0.072(2)
	χ^2	0.977
	R_p	4.28%
	R_{wp}	5.16%

this sample was 1:0.25:0.75 (Ba:Bi:Co). (As will be discussed later, this amount of $BaCoO_3$, does not significantly influence the physical properties of $BaBi_{0.28}Co_{0.72}O_{2.2}$.) Substantial oxygen deficiency is similar to what has been previously observed in cubic $BaCoO_{2.23}$ [3]. We have no information about how this high oxygen deficiency is accommodated by the Bi–O and Co–O coordination polyhedra: the vacancies may be either truly randomly arranged, or they may occur in specific coordination environments (eg CoO_4 squares or CoO_5 pyramids) that are randomly arranged. This highly oxygen deficient material also appears to be similar to what is seen in the $Ba_{1-x}Sr_xCoO_3$ system [6], where a cubic phase made in nitrogen atmosphere for Sr content $0.2 \leqslant x \leqslant 0.5$ appeared to be a single phase highly oxygen deficient cubic material that did not show the presence of short or long range vacancy ordering. Our electron diffraction data for $BaBi_{0.28}Co_{0.72}O_{2.2}$ indicate the presence of short range ordering of Bi/Co and O vacancies. The broad features present in the neutron powder pattern (figure 4) are attributed to the diffuse scattering from this short range ordering. Thus neutron powder diffraction confirms the average structure of the new, highly oxygen deficient phase, with a refined stoichiometry of $BaBi_{0.28}Co_{0.72}O_{2.2}$.

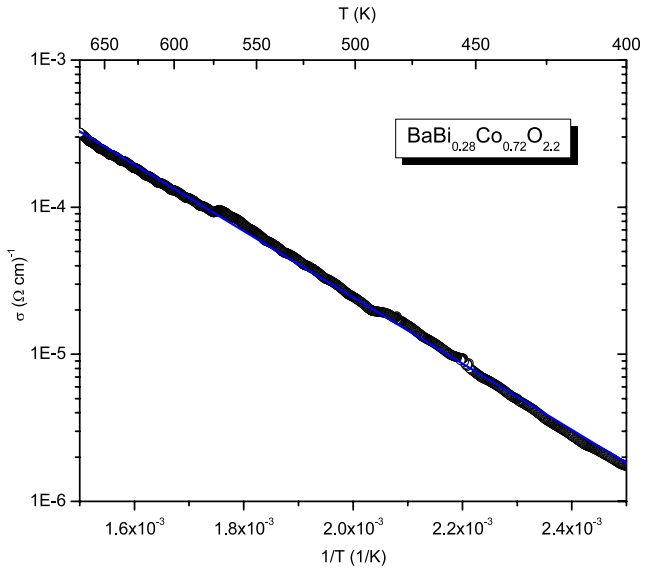

Figure 5. The DC electrical conductivity of $BaBi_{0.28}Co_{0.72}O_{2.2}$ versus reciprocal temperature.

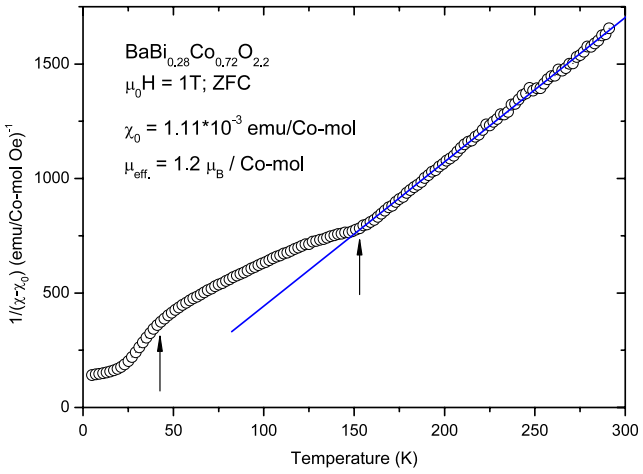

Figure 6. Inverse of magnetic susceptibility $(1/(\chi - \chi_0))$ versus temperature of $BaBi_{0.28}Co_{0.72}O_{2.2}$. The solid line represents the Curie–Weiss fit. The two arrows indicate the temperatures discussed in text.

4. Physical properties

We measured the temperature dependence of the conductivity of $BaBi_{0.28}Co_{0.72}O_{2.2}$. Semiconducting behavior, and the validity of the simple relation $\sigma = \sigma_0 \exp(-E_g/2k_BT)$, where σ is electrical conductivity and E_g activation energy, are shown in figure 5. From the fit we obtained a transport activation energy E_g equal to 1.8 eV. Previous studies on both parent compounds have indicated that they are semiconductors as well [6, 11, 12]. More detailed study, for instance spectroscopy measurements, to understand the electronic configuration of $BaBi_{0.28}Co_{0.72}O_{2.2}$ may be of interest.

The inverse magnetic susceptibility versus temperature behavior of $BaBi_{0.28}Co_{0.72}O_{2.2}$ is shown in figure 6. In the high temperature region, above 150 K, a linear relationship is found, and the effective moment (μ_{eff}) and the Weiss temperature (Θ_W) can be fitted. The solid line represents the least square fit to the Curie–Weiss model with $\mu_{\text{eff}} = 1.2\ \mu_B$/Co-mol and $\Theta_W = 33$ K. The effective magnetic moment may be slightly overestimated due to the presence of 3 wt% $BaCoO_3$ impurity. Based on Rietveld analysis, the stoichiometry of our sample is $BaBi_{0.28}Co_{0.72}O_{2.2}$. Making the assumption consistent with expectations that Bi is present only as the Bi^{3+} ion[6], the Co oxidation state in our compound will be slightly more than +2 (2.07). Because the low spin Co^{2+} state yields a magnetic moment of 1.732 μ_B/mol-Co, comparing with observed effective magnetic moment 1.2 μ_B/Co-mol, we conclude that some fraction of low spin (non-magnetic) Co^{3+} is present in $BaBi_{0.28}Co_{0.72}O_{2.2}$.

There are two characteristic temperatures marked on figure 6. Above 150 K the inverse of magnetic susceptibility $(1/\chi)$ is proportional to T, and the positive value of the Weiss temperature means that ferromagnetic interactions are dominant for $T > 150$ K. Below 150 K, some antiferromagnetic correlations and possibly short range ordering of the spins occurs, which is manifested by increase of $1/\chi$ (χ decreases) as temperature decreases. Antiferromagnetic interactions ($T_N = 15$ K) were recently investigated by neutron diffraction and μSR in $BaCoO_3$ [13]. Ferromagnetic interactions in $BaBi_{0.28}Co_{0.72}O_{2.2}$ are responsible for the rapid decrease of $1/\chi$ below 40 K (see the arrow on figure 6). Competing antiferromagnetic and ferromagnetic interactions leads to frustration, which often causes spin-glass ordering in cobaltates [14–23]. In order to test for the presence of a spin-glass, cluster-glass, or superparamagnetic phase in $BaBi_{0.28}Co_{0.72}O_{2.2}$, ac and dc magnetic measurements were performed.

The temperature dependence of the dc magnetic susceptibility was measured at a magnetic field of 0.01, 0.1 and 1 T (figure 7) on heating, after cooling without a magnetic field (ZFC) and with a magnetic field (FC). As temperature increases, the ZFC magnetic susceptibility reaches a maximum (T_{max}) value and then decreases. The data show that the T_{max} temperature and $\chi(T_{\text{max}})$ strongly depend on applied magnetic field, which is rather typical for a cluster-glass. In this scenario, the maximum is an outcome of the competition between the applied magnetic field and local magnetization orientations of individual Co clusters [24].

The presence of Bi atoms, and non-magnetic Co^{3+}, blocks long range chemical ordering, so it is not visible on electron diffraction patterns and in magnetic measurements; similarly, the distribution of non-magnetic Co^{3+} ions in the chains of $BaCoO_3$ [25] has been postulated to disturb the occurrence of long range magnetic order in that phase. A maximum in $\chi(T)$ is not observed in field cooling (FC) measurement and a large splitting of the ZFC and FC magnetization curves is observed, as shown in the inset of figure 7. Under an applied field of 0.01 T, the FC and ZFC lines merge at about $T_R = 25$ K. This temperature determines an upper limit of an irreversibility

[6] The assumption that Bi oxidation state is +5 makes the Co oxidation state +1.4 and therefore is non-realistic.

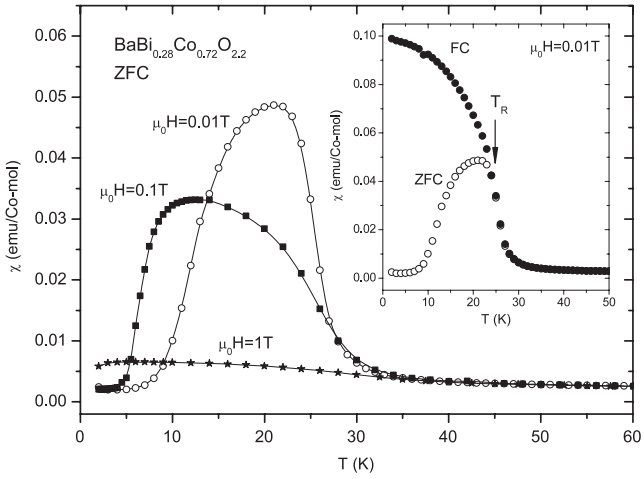

Figure 7. ZFC magnetic susceptibility χ of $BaBi_{0.28}Co_{0.72}O_{2.2}$ versus temperature under magnetic fields of 0.01 (circles), 0.1 (squares) and 1 T (asterisks). The inset shows the ZFC (open circles) and FC (close circles) curves of χ under a magnetic field of 0.01 T.

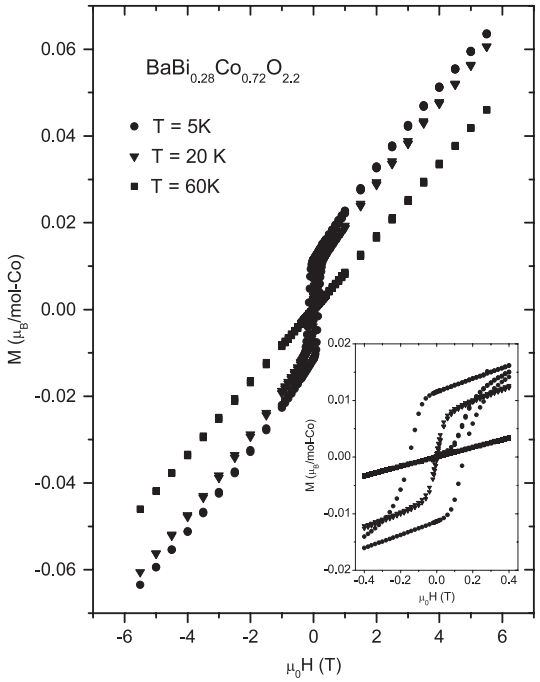

Figure 8. The magnetic hysteresis loops measured for $BaBi_{0.28}Co_{0.72}O_{2.2}$ at 5 K (circles), 20 K (triangles), and 60 K (squares). The inset shows more details of the magnetic hysteresis loops.

region and is called the blocking temperature and depends on the size of magnetic clusters, the anisotropy constant of the material, the applied field and on measuring time [7, 26]. Although a broad maximum of the ZFC line is typical for both spin-glass and cluster-glass materials, the monotonic increase of the FC line (with decreasing temperature) is characteristic for cluster-glass compounds [24, 27, 28]. This is opposite to what is observed in spin-glass compounds, in which a small cusp in the FC behavior is often visible [28, 29]. This observation is confirmed in the ac measurement discussed later.

Figure 8 shows the magnetization loops measured at 5, 20, and 60 K. At the highest temperature, $M(H)$ remains a straight line over the whole applied magnetic field region. It is clear that M versus H does not saturate, even at the highest magnetic field (5.5 T). The inset shows the open hysteresis loop at 5 K and the coercive magnetic field, about 1500 Oe, indicates that $BaBi_{0.28}Co_{0.72}O_{2.2}$ is relatively hard magnetic material. Because one of the criteria for superparamagnetism is the observation of an $M(H)$ curve without hysteresis [30], we conclude that superparamagnetism is not present in $BaBi_{0.28}Co_{0.72}O_{2.2}$. The remanence magnetic field, measured at $T = 5$ K, reaches ± 0.01 μ_B/mol-Co. An almost identical value has been obtained for pure $BaCoO_3$ ([6]); therefore, the hysteresis loop in $BaBi_{0.28}Co_{0.72}O_{2.2}$ cannot originate from the presence of less than 3 wt% $BaCoO_3$ impurity, a material in which the appearance of single-domain FM clusters is suggested [31].

Finally we measured the ac magnetic susceptibility in the temperature range 17–40 K, $H_{AC} = 2$ Oe and at frequencies $f = 1, 10, 100, 1000$ Hz. The maximum of the real part of the magnetic susceptibility appears at about $T_f = 25.5$ K (see main panel of figure 9), which is close to the blocking temperature, T_R (see the inset of figure 7). The carefully determined freezing temperature (T_f) shifts slightly with frequency, and our experimental data can be fitted by the empirical Vogel–Fulcher formula: $\tau = 1/f = \tau_0 \exp(\frac{E_a}{k_B(T_f - T_0)})$, where τ_0 is an intrinsic relaxation time, E_a is an activation energy, T_0 is

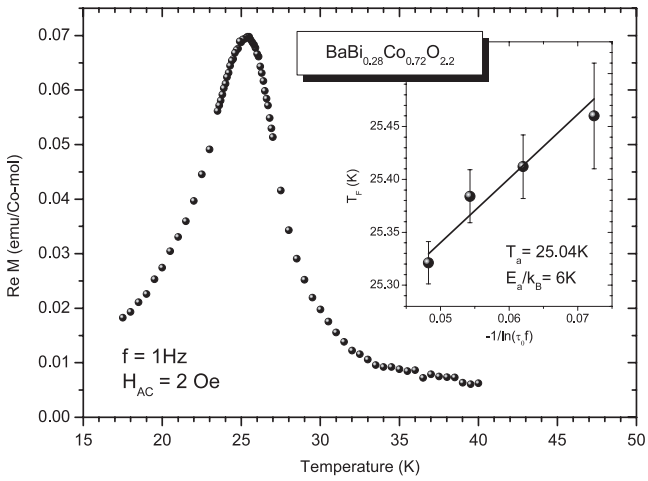

Figure 9. Temperature dependence of the real part of the AC susceptibility ($f = 1$ Hz, $H_{AC} = 2$ Oe). The inset shows the fit to the Vogel–Fulcher law, assuming the relaxation time $\tau_0 = 10^{-9}$ s.

the Vogel–Fulcher temperature [32, 33]. After modification of the above equation, one can obtain a simple relation between T_f and f: $T_f = T_0 - \frac{E_a}{k_B}\frac{1}{\ln(\tau_0 f)}$, with three fitting parameters: T_0, E_a and τ_0. The intrinsic relaxation time, τ_0, can vary from 10^{-7} s, found in $Co_{0.2}Zn_{0.8}Fe_2O_4$ cluster-glass compound [34], to 10^{-13} s typical for spin-glass compounds [35]. We did not obtain a physically meaningful result when all three parameters were varied freely. This is most likely caused by the fact that in our study we have only four experimental points. Reasonable results were achieved for fixed τ_0 and fitted T_0 and E_a. For $\tau_0 = 10^{-9}$ s the fit of Vogel–Fulcher equation yields: $T_0 =$

25.04 ± 0.06 K and $E_a/k_B = 6 \pm 1$ K. Assuming a four order of magnitude shorter time: $\tau_0 = 10^{-13}$ s, we obtained $T_0 = 24.87 \pm 0.08$ K and $E_a/k_B = 14 \pm 2$ K. The very low activation energy in $BaBi_{0.28}Co_{0.72}O_{2.2}$ reflects the fact that T_f changes only 0.14 K when the frequency changes by three orders of magnitude. For spin glasses materials the relative shift per frequency decade, $\delta T_f = \Delta T_f/(T_f \Delta \log(f))$, is often calculated. In $BaBi_{0.28}Co_{0.72}O_{2.2}$ we estimate $\delta T_f = 0.002$, which is an order of magnitude smaller than for spin-glass systems: 0.025 (URh_2Ge_2) [36], 0.016 (Ce_2CuGe_3) [37], but comparable to 0.005 reported for cluster-glass U_2IrSi_3 [40] and CuMn, which is an example of a canonical spin-glass compound [33]. The activation energy E_a is $0.24k_BT_f$ or $0.55k_BT_f$ for $\tau_0 = 10^{-9}$ s and 10^{-13} s respectively. Both values are much smaller than obtained for spin-glass compounds: e.g. Fe_2TiO_5 ($3.4k_BT_f$) [38], and U_2MSi_3 (6–$10k_BT_f$), where M = Pd, Pt, Au [39], and is also smaller than estimated for cluster-glass compounds: U_2IrSi_3 ($1.6k_BT_f$) [40], UCuGe($1.5k_BT_f$) [41], and $Co_{0.2}Zn_{0.8}Fe_2O_4$ ($0.77k_BT_f$) [34]. This comparison strongly suggest the formation of the FM cluster-glass state in $BaBi_{0.28}Co_{0.72}O_{2.2}$ below T_f.

5. Conclusions

In the perovskites, magnetic and/or electrical phase separation is frequently observed, a characteristic that can explain many of their interesting properties. Here we propose cluster-glass behavior in the new perovskite $BaBi_{0.28}Co_{0.72}O_{2.2}$ based on its frequency dependent ac magnetic properties and ZFC and FC dc magnetization. The cluster-glass behavior may have its origin in the formation of interacting ferromagnetic clusters. The electron diffraction study confirms the existence of short range ordering in this phase. We propose a nanoscale phase separation scenario, perhaps with different ratios of Bi:Co present in very small regions of the material, yielding the existence of magnetic clusters in $BaBi_{0.28}Co_{0.72}O_{2.2}$. Because cubic $BaBi_{1-x}Co_xO_{3-\delta}$ forms in the range $0.7 < x < 0.9$, we believe that the size of the clusters can be tuned by both cobalt and oxygen concentration. As a result, the physical properties, e.g. activation energy and freezing temperature, can be expected to change with composition and annealing conditions. Cold-neutron elastic and inelastic scattering study on $BaBi_{0.28}Co_{0.72}O_{2.2}$ would be of interest in future studies, as these techniques have provided indirect evidence of existing nanomagnetic droplets in $La_{1-x}Sr_xCoO_3$ [42].

Acknowledgments

This research was supported by the US Department of Energy, Basic Energy Sciences, grant DE FG02-98-ER45706. T M McQueen gratefully acknowledges support by the National Science Foundation Graduate Research Fellowship Program. Work at Los Alamos was performed under the auspices of the US DOE.

References

[1] Wold A and Ward R 1954 *J. Am. Chem. Soc.* **76** 1029–30
[2] Nakatsuka A, Yoshiasa A, Nakayama N, Mizota T and Takei H 2004 *Acta Crystallogr.* C **60** i59–60
[3] Strauss S W, Fankuchen I and Ward R 1951 *J. Am. Chem. Soc.* **73** 5084–6
[4] Rice J and Wang Y R 1989 *Physica* C **157** 192
[5] Felser C, Yamaura K and Cava R J 1999 *J. Solid State Chem.* **146** 411
[6] Yamaura K, Zandbergen H W, Abe K and Cava R J 1999 *J. Solid State Chem.* **146** 96–102
[7] Pardo V, Rivas J, Baldomir D, Iglesias M, Blaha P, Schwarz K and Arias J E 2004 *Phys. Rev.* B **70** 212404
[8] Toby B H 2001 *J. Appl. Crystallogr.* **34** 210
[9] Larson A C and Von Dreele R B 2000 *Los Alamos National Laboratory Report LAUR* p 86
[10] Vincent H, Perrier Ch, L'hertier Ph and Labeyrie M 1993 *Mater. Res. Bull.* **28** 951
[11] Raghu N, Ravi V and Kutty T R N 1991 *Mater. Res. Bull.* **26** 261
[12] Rice M J and Wang Y R 1989 *Physica* C **157** 192
[13] Nozaki H, Janoschek M, Roessli B, Sugiyama J, Keller L, Brewer J H, Ansaldo E J, Morris G D, Takami T and Ikuta H 2007 *Phys. Rev.* B **76** 014402
[14] Asai K, Yokokura O, Nishimori N, Chou H, Tranquada J M, Shirane G, Higuchi S, Okajima Y and Kohn K 1994 *Phys. Rev.* B **50** 3025
[15] Yamaguchi S, Okimoto Y and Tokura Y 1997 *Phys. Rev.* B **55** R8666
[16] Zobel C, Kriener M, Bruns D, Baier J, Gruninger M/, Lorenz T, Reutler P and Revcolevschi A 2002 *Phys. Rev.* B **66** 020402
[17] Wu J and Leighton C 2003 *Phys. Rev.* B **67** 174408
[18] Tokura Y, Okimoto Y, Yamaguchi S, Taniguchi H, Kimura T and Takagi H 1998 *Phys. Rev.* B **58** R1699
[19] Caciuffo R, Rinaldi D, Barucca G, Mira J, Rivas J, Senaris-Rodrigues M A, Radaelli R G, Floriani D and Goodenough J B 1999 *Phys. Rev.* B **59** 1068
[20] Mukherjee S, Ranganathan R, Anilkumar P S and Joy P A 1996 *Phys. Rev.* B **54** 9267
[21] Nam D N H, Jonason K, Nordblad P, Khiem N V and Phuc N X 1999 *Phys. Rev.* B **59** 4189
[22] Prokhorov V G, Lee Y P, Kim K W, Ishchuk V M and Chukanova I N 2002 *Phys. Rev.* B **66** 132410
[23] Itoh M, Natori I, Kubota S and Motoya K 1995 *J. Magn. Magn. Mater.* **140–144** 1811
[24] Szymczak H, Baran M, Babonas G J, Diduszko R, Fink-Finowicki J and Szymczak R J 2005 *J. Magn. Magn. Mater.* **285** 386
[25] Yamaura K and Cava R J 2000 *Solid State Commun.* **115** 301–5
[26] Almeida D and Thouless D 1978 *J. Phys. A: Math. Gen.* **11** 983
[27] Anil Kumar P S, Joy P A and Date S K 1998 *J. Phys.: Condens. Matter* **10** L487
[28] Itoh M, Natori I, Kubota S and Motoya K 1994 *J. Phys. Soc. Japan* **63** 1486
[29] Süllow S, Nieuwenhuys G J, Menovsky A A, Mydosh J A, Mentink S A M, Mason T E and Buyers W J L 1997 *Phys. Rev. Lett.* **78** 354
[30] Bean C P and Livingston J D 1959 *J. Appl. Phys.* **30** 120S
[31] Botta P M, Pardo V, Baldomir D, de la Calle C, Alonso J A and Rivas J 2006 *Phys. Rev.* B **74** 214415
[32] Fulcher G I 1925 *J. Am. Ceram. Soc.* **8** 339
Fulcher G I 1925 *J. Am. Ceram. Soc.* **8** 789
[33] Mydosh J A 1993 *Spin Glasses: an Experimental Introduction* (London: Taylor and Francis)
[34] Bhowmik R N and Ranganathan R 2002 *J. Magn. Magn. Mater.* **248** 101
[35] Tholence J L 1980 *Solid State Commun.* **35** 113
[36] Süllow S, Nieuwenhuys G J, Menovsky A A, Mydosh J A, Mentink S A M, Mason T E and Buyers W J L 1997 *Phys. Rev. Lett.* **78** 355
[37] Tien C, Feng C H, Wur C S and Lu J J 2000 *Phys. Rev.* B **61** 12151

[38] Tholence J L, Yeshurun Y, Kjems J K and Wanklyn B 1986 *J. Magn. Magn. Mater.* **54–57** 203
[39] Li D, Shiokawa Y, Haga Y, Yamamoto E and Onuki Y 2002 *J. Phys. Soc. Japan* **71** 418
[40] Li D, Nimori S, Shiokawa Y, Haga Y, Yamamoto E and Onuki Y 2003 *Phys. Rev.* B **68** 172405
[41] Tran V H, Zaleski A J, Troć R and Du Plessis P De V 1996 *J. Magn. Magn. Mater.* **162** 247
[42] Phelan D, Louca D, Rosenkranz S, Lee S-H, Qiu Y, Chupas P J, Osborn R, Zheng H, Mitchell J F, Copley J R D, Sarrao J L and Moritomo Y 2006 *Phys. Rev. Lett.* **96** 027201